Pergamon

PII: S0967-0645(96)00039-2

Deep-Sea Research II, Vol. 43, No. 7-8, pp. 1971-2001, 1996

0967-0645/96 $15.00 + 0.00

Acoustical study of the spatial distribution of plankton on Georges Bank and the relationship between volume backscattering strength and the taxonomic composition of the plankton

P. H. WIEBE,* D. G. MOUNTAIN,† T. K. STANTON,* C. H. GREENE,‡ G. LOUGH,† S. KAARTVEDT,§ J. DAWSON¶ and N. COPLEY*

(*Received* 13 *December* 1994; *in revised form* 5 *February* 1996; *accepted* 30 *April* 1996)

Abstract—High frequency (420 kHz) sound was used to study the volume backscattering from plankton and micronekton over Georges Bank as part of a study designed to determine the correlation length scales of plankton spatial patterns in relation to physical structure and to intercompare different kinds of sampling and remote-sensing instrumentation. Two physically distinct areas were studied: a well-mixed area in a shallow portion of the Bank and a stratified area on the deeper southern flank of the Bank. A submersible echo sounder with a down-looking transducer was mounted in a towed V-fin. Volume backscattering data were collected from near the sea surface to the bottom (40–80 m).

Vertical and horizontal volume backscattering structure in the stratified region differed from that in the well-mixed area in both mean and variance, providing evidence that physical forcing of the pattern varied significantly between the two areas. Internal waves appeared to modulate the depth of dense mid-depth volume scattering layers in the stratified sites. In the mixed area, there was little horizontal layering or coarse-scale horizontal structure. However, fine-scale vertical lineations were evident with horizontal length scales on the order of the depth of the water column. One hypothesis to explain these vertical lineations in the well-mixed areas involves the development of secondary vertical circulation cells associated with the tidal flows over a rough bottom. Although volume backscattering at the stratified sites was 4–7 times higher than at the mixed site, there was no significant difference in MOCNESS (Multiple Opening/Closing Net and Environmental Sensing System) collected biovolumes between these locations. The difference in volume backscattering was due to differences in both the acoustic scattering properties of zooplankton taxa and the taxonomic composition of the plankton between the sites. Correlations between taxon abundance and volume scattering were positive and significant only for pteropods and euphausiid larvae. The abundances of copepods, chaetognaths, fish larvae, and amphipods were not significantly correlated with volume scattering. When taxon-specific model predictions of acoustic backscattering cross-section, developed by Stanton *et al.* (*ICES Journal of Marine Science*, **51** (1994) 505–512), were used with field collected individual size and abundance data to predict measured volume backscattering data, good agreement was found between observed and predicted volume backscattering strengths.

* Woods Hole Oceanographic Institution, Woods Hole, MA 02543, U.S.A.
† National Marine Fisheries Service, Woods Hole, MA, U.S.A.
‡ Cornell University, Ithaca, New York, U.S.A.
§ Biology Department, University of Oslo, Oslo, Norway.
¶ BioSonics Inc., Seattle, WA, U.S.A.

INTRODUCTION

Georges Bank is a highly productive, physically and biologically active region. Across the Bank, there are substantial physical differences in water column stability resulting from the interaction between water column depth and tidal currents. In the area over the Bank where the bottom depths are less than 60 m, the water column remains well mixed all year (Garrett *et al.*, 1978; Flagg, 1987). The deeper portions of the Bank (> 60 m) also are well mixed during winter, due to the combined effects of wind- and tidal-driven mixing, and surface cooling. Increased surface warming during the spring leads to thermal and density stratification over the deeper portions of the Bank. The importance of vernal stratification to the survival and growth of larvae of cod (*Gadus morhua*) and haddock (*Melanogrammus aeglefinus*) and their associated predators and prey was the focus of a two-ship study in May 1992. During this study, a variety of sampling strategies and instrumentation systems were used to determine the spatial structure of biological and physical variables in the well-mixed and stratified portions of the Bank. This study also was designed to enable comparisons among the different kinds of instrumentation, some conventional and some based on new technology.

As part of this stratification study, we mapped the distribution of zooplankton at selected study sites on the southern flank of Georges Bank using a towed body that contained a 420 kHz dual-beam acoustics system (Wiebe and Greene, 1994). Our specific objectives were (i) to make high-resolution 2-D and 3-D acoustical visualizations of the vertical and horizontal distribution of zooplankton at three major study sites [a Fixed Mooring Site (FMS), a Drogue Site (DS), and a Well-Mixed Site (WMS)], (ii) to compare these data with plankton biovolumes and taxon numbers determined from plankton samples collected with Multiple Opening/Closing Net and Environmental Sensing System (MOCNESS; Wiebe *et al.*, 1985), and (iii) to study the variations in volume backscattering associated with hydrographic changes on the Bank's southern flank.

METHODS

Sampling on Georges Bank was conducted during a two-ship operation involving the R.V. *Albatross IV* and the R.V. *Endeavor* during the period 17–28 May 1992. The work reported herein was done from the R.V. *Albatross IV* utilizing the following instrument systems.

High-frequency acoustic system

A dual-beam, 420-kHz echo sounder, specially designed by BioSonics Inc., was mounted in an ENDECO V-finned towed body (see Fig. 8 in Wiebe and Greene, 1994). The transducer was mounted inside the towed body and oriented vertically (downlooking) through an open cut-out on the aluminum bottom panel. In this configuration, it was used to map the fine-scale vertical patterns of acoustic backscatter along the ship's trackline. During some tows, a MOCNESS or CTD also was deployed. Volume backscattering data were collected routinely from 5 m to the bottom (usually 40–80 m). Given the gain setting used in configuring the acoustic system, the effective maximum depth for quantitative work was 50 m. Data from this sounder were observed on an oscilloscope and processed by a computer in real-time; the analog signals from the echo sounder were recorded on a Sony

Table 1. *Calibration data for towed* 420 *kHz echo sounder*

Parameter	Value
Transducer nominal beamwidth	narrow beam = 6° wide beam = 15°
Directivity index	29.903
Wide beam drop-off	1.167
Mean beam pattern factor (b_{AV}^2)	0.001001
Source level (re: 1 μPa at 1 m)	220.143
Receiving sensitivity (re: 1 V/μPa):	
40log$R$	
NB	−163.442
WB	−167.738
20log$R$	
NB	−154.772
WB	−158.916
Receiver gain setting	+12
A (Integration scaling constant)	12.0084E−5

DAT tape recorder for post-processing of selected grid studies and transect lines. The towed body also was equipped with a MOCNESS CTD package that provided measurements of depth, temperature, conductivity, and fluorescence.

The overall dimensions of the towed body are: length: 139.7 cm; width at front: 66 cm; width at rear: 142.2 cm; height: 48.26 cm. It is constructed primarily of fiberglass. A thick aluminum disk forms the bottom of the towed body and provides the foundation for mounting instrument pressure cases. For this work, four pressure cases were mounted on top of the aluminum disk. One case contained the battery to run the MOCNESS sensor electronics, the second contained the MOCNESS electronics, the third contained the sounder electronics, and the fourth contained a SeaTech Fluorometer. A stainless steel bracket attached at three mid-section points (top and each side) extended forward 28 cm beyond the nose of the towed body and was used to support the temperature, conductivity, and fluorescence sensors. A single tow point at the top allows for bi-directional motion of the towed body (roll and pitch).

The sounder was calibrated in the BioSonics calibration facility in Seattle, WA before the cruise. Calibration data included system performance parameters for source level, receiver sensitivity, and transducer beam pattern (Table 1). The ping duration of the sounder was 0.3 ms. With this pulse length, single targets could be resolved if their distances from the transducer were different by approximately 22 cm. Unfortunately, this was not often the case, so this study uses only the volume scattering data as measured with a single 6° beam. The data were stored in 2-D files of depth versus along-track position for analyses.

Both the logarithmic form of scattering, S_v (volume backscattering strength), and the linear form, s_v (volume backscattering coefficient) were analyzed. The two quantities are related by the following equation (Clay and Medwin, 1977):

$$S_v \equiv 10\log(s_v) \tag{1}$$

The dimensions of s_v are m^{-1} and are suppressed.

MOCNESS sampling procedures

Sampling for fish larvae and zooplankton was conducted using a 1-m^2 MOCNESS equipped with 335 μm mesh nets (Lough and Potter, 1993). At the Well-Mixed Site, where the bottom was about 40 m, a double oblique tow was usually made with nets 1–4 sampling 10 m intervals from the bottom to the surface and nets 5–8 sampling 10 m intervals from the surface to the bottom. At the Fixed Mooring and Drogue Sites, where water depths were 70–80 m, 10 m intervals from the bottom to the surface were usually sampled. Each net filtered about 250 m^3 of water. Net samples were preserved in a 4% formaldehyde–seawater solution. Data from 21 MOCNESS tows were used in this analysis (Table 2).

CTD data collection and analysis

CTD data were collected with a Neil Brown Instrument Systems MK5 CTD equipped with a SeaTech fluorometer. The data were processed to 1 db average values of pressure, temperature, salinity, and fluore cence. The fluorometer data were voltage measurements (0–5 volts full scale). No attempt was made to convert the voltage measures to chlorophyll values, although subsequent comparison of the fluorometer values with extracted chlorophyll samples indicated a linear relationship. During long transects conducted across the Bank, the CTD was lowered or raised through the water column approximately every 12 min as the vessel steamed about 83 m min^{-1} (2.5 kts). Each up or down cast required 1–2 min to complete. This resulted in discrete vertical profiles approximately every kilometer along the track.

Fixed mooring and drogue sites data collection and analysis

A mooring was deployed on the southern flank of Georges Bank during the May 1992 cruise to measure the water column conditions in the stratified region during the study period. The mooring, deployed on May 21 and recovered on May 27, was located at 40°42.29′N, 67°52.33′W where the water depth was 80 m (Fig. 1). Vector-Measuring Current Meters (VMCMs), recording every 3.75 min, were located at 15 and 45 m depths. Temperature/conductivity recorders (SeaBird SeaCat SBE 19 instruments) were located at 1, 10, 20, 30 and 40 m depths. Temperature recorders (Branker Tpod instruments) were located at 5, 25 and 35 m depths. The SeaCats and Tpods recorded every 2 min. The data records from all of the moored instruments were processed to hourly averaged values. The "raw" temperature records also were high pass filtered using a Butterworth filter with a 40 min cutoff for analysis of the high frequency variability in temperature (Parks and Burrus, 1987).

Shortly after the mooring was put in place, a set of three surface drifters with subsurface drogues were released at the fixed site. One of the drifters had a Loran-C tracking device, and the R.V. *Albatross* had a unit to receive its position. As expected, the drogues moved to the southwest and repeated cross-stream transects comparable to the fixed location sections were made relative to the drogue.

Field sampling on the Georges Bank southern flank

A mobile acoustic surveying program was designed to provide information about the fine- to meso-scale spatial distributions of volume backscattering strength at 420 kHz in the

Table 2. Summary of towed acoustic system deployments during the Georges Bank stratification study aboard R.V. Albatross IV *cruise* 92–05, 19–29 *May* 1992. *Acoustic data from each of these deployments and data from the listed MOCNESS tows were used in this paper*

Towed body tow number	Lat. °N start/end positions	Long. °W start/end positions	Local date/time (GMT + 4 h) (start/end)	Station area*
14	40 57.46 41 00.03	67 01.87 68 01.80	22 May 02:48–03:51	With MOCNESS 975 @ WMS
15	40 56.85 41 01.28	68 01.84 68 01.62	22 May 04:38–06:48	With CTD @ WMS
16	40 40.92 40 43.98	67 52.33 67 51.80	22 May 13:19–14:27	With MOCNESS 977 @ FMS
17	40 40.64 40 45.31	67 52.30 67 50.50	22 May 15:07–16:48	With CTD @ FMS
18	40 40.20 40 42.54	67 15.75 67 51.81	22 May 21:07–22:24	With MOCNESS 979 @ FMS
19	40 40.58 40 45.36	67 52.74 67 52.76	22–23 May 23:10–01:05	With CTD @ FMS
20	40 58.29 41 01.22	68 01.95 68 01.68	23 May 02:41–03:43	With MOCNESS 980 @ WMS
21	40 57.23 40 00.78	68 01.71 68 01.32	23 May 04:52–06:21	With CTD @ WMS (short tow)
22	40 38.67 40 40.74	68 05.35 68 07.26	23 May 11:21–12:24	With MOCNESS 982 @ DS
23	40 40.15 40 44.95	68 06.56 68 06.96	23 May 13:45–15:04	With CTD @ DS
24	40 41.54 40 43.11	68 07.92 68 07.17	23 May 17:10–18:03	With MOCNESS 984 @ DS with *Endeavor*
25	40 41.34 40 45.01	68 07.68 68 07.58	23 May 18:40–20:43	Transect tow with CTD @ DS with *Endeavor*
26	40 57.04 40 59.96	68 02.05 68 01.91	23 May 22:09–23:52	With MOCNESS 985 @ WMS
27	40 39.21 40 41.50	68 09.83 68 10.20	24 May 02:27–03:21	With MOCNESS 987 @ DS with *Endeavor*
29	40 39.72 40 41.55	68 12.93 68 12.18	24 May 12:46–16:31	GRID I tow with 6 legs @ DS with *Endeavor*; leg 6 with MOCNESS 990; legs 3, 4, 5 with CTD
31	40 42.64 40 58.98	67 51.69 68 01.90	24 May 22:41–04:13	Transect tow with CTD from FMS to WMS; (seas rough)
32	40 42.49 40 40.33	67 52.94 67 50.69	25 May 10:33–15:51	GRID II tow with 5 legs @ FMS with *Endeavor*; LEGS 1 & 5 with MOCNESS 991 & 992; legs 2,3,4 with CTD; (very rough seas)

(continued)

Table 2. Continued

Towed body tow number	Lat. °N start/end positions	Long. °W start/end positions	Local date/time (GMT + 4 h) (start/end)	Station area*
33	40 58.86 40 54.90	68 00.72 68 03.21	26 May 08:59–13:11	GRID IV tow with 6 legs @ WMS; legs 1 & 6 with MOCNESS 993 & 994; legs 2–4 with CTD; (seas moderated); Grid III done only by *Endeavor*
34	40 42.53 40 42.36	67 51.51 67 51.37	26 May 17:57–20:21	BIOSPAR/GB comparison hove-to time-series @ FMS
35	40 59.34	68 00.95	26–27 May 22:53–03:08	GRID V tow with 6 legs @ WMS with *Endeavor*; legs 1 & 6 with MOCNESS 997 & 998; legs 3, 4, 5 with CTD
36	40 28.79 40 47.81	68 20.81 68 35.34	27–28 May 17:44–06:06	Cross-shelf transect on southern flank of Georges Bank west of main work site with CTD and MOCNESS tows 1000, 1001, 1002, & 1004.
37	40 40.99 40 51.03	68 37.85 68 49.57	28 May 13:03–16:33	Southwestern Bank to Great South Channel transect with CTD and MOCNESS tows 1005 & 1006

*FMS, Fixed Mooring Site; DS, Drogue Site; WMS, Well-Mixed Site.

vicinity of the MOCNESS towing. This sampling was coordinated with the deployment of other instruments from the R.V. *Endeavor* when joint ship operations were being conducted (Fig. 1 and Table 2).

On most of the acoustic transects, data were integrated over 30-s intervals in 2 m depth strata. Thus, based on a ship speed of 2 kts, the minimum resolution distance on transect sampling was approximately 30 m.

Twenty-eight deployments of the towed acoustic system were made of which 22 were used in this analysis (Table 2). These 22 tows successfully acquired high resolution data on the vertical and horizontal distribution of zooplankton primarily at the Fixed Mooring (6), the Drogue (6), and the Well-mixed (7) sites. At these main work sites, a series of transects was conducted approximately perpendicular to the bathymetry (Fig. 1). There were three longer transects. One transect (GB31) extended from the FMS to the WMS, a distance of about 28 km. A second transect (GB36) crossed the southern shelf west of the main work area (distance = 54.9 km), and a third (GB37—distance = 18.1 km) ran from the Bank into the Great South Channel (Fig. 1). Acoustical measurements were made continuously along the tracklines. In addition, time-series acoustical measurements were made at the FMS with the ship hove-to next to the mooring.

MOCNESS tows were taken during a portion of about half of the acoustic transects for comparison of the net collected biovolume and species composition with the acoustic data. The track line of the net system was displaced to the port side of the vessel about 5 m from that of the towed acoustic system and the net setback (displacement aft of the ship), relative to the towed acoustic system, ranged from about −45 m to +5 m depending upon MOCNESS depth. For each net, acoustical volume backscattering data were extracted from

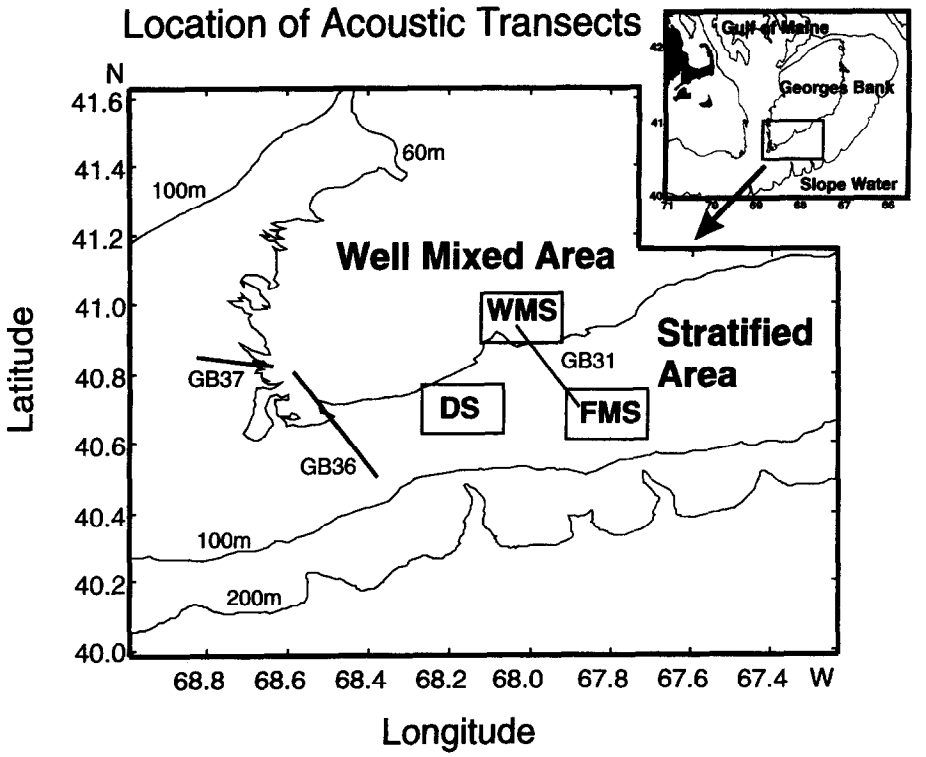

Fig. 1. Position of the acoustical transects, MOCNESS tows, CTD towyos, and the mooring in relation to the topography of Georges Bank. At the Fixed Mooring Site were the mooring and acoustic tows GB16, 17, 18, 19, 32 and 34; at the Drogue Site (DS) were acoustic tows GB22, 23, 24, 25, 27, and 29; at the Well-Mixed Site were acoustic tows GB14, 15, 20, 21, 26, 33, and 35. Long transects GB31, and GB36 went from the stratified region to the well-mixed region of the Bank; GB37 was in a well-mixed area of the Great South Channel. See Table 2 for acoustic, CTD, and MOCNESS tow pairings. Both the Fixed Mooring Site and the Drogue site were in the Stratified region. Sixty, 100 and 200 m isobaths are shown.

the acoustical record based on the depth strata sampled and the time the net was open. With a net open for 5 or more minutes, errors associated with offsets in matching the acoustic record with the trajectory of the net were minor.

Sample biomass and silhouette description

For comparison with the acoustics data, total biovolume was measured on 109 MOCNESS samples using the displacement volume method (Wiebe, 1988; Wiebe *et al.*, 1975). The size frequency of individuals as a function of taxon also was determined for 21 of these samples (7 from the WMS-tows 975[3]; 998[4], 10 from the DS-tows 982[5]; 990[5], and 4 from the FMS-991[4]) using the silhouette method described by Davis and Wiebe (1985). The length measurements were converted to wet weights using length-to-wet-weight algorithms mostly from Davis and Wiebe (1985). Algorithms for several new categories were developed during the course of this or earlier work (unpublished). The wet weights were used for comparisons of the contribution of each taxon to the total estimated biomass. The length measurements were used directly in the acoustic models described below.

Spatial spectral analysis of data

Variance spectra of the along-track acoustics, temperature, and fluorescence data from the towed acoustic system were calculated for transects GB31, GB36 and GB37. In the case of the acoustic fields, a Fast Fourier Transform (FFT) was calculated for the horizontal spatial series of volume backscattering coefficient (s_v) for each of the top 18 (upper 36 m) horizontal depth strata. These were then averaged by spatial wavenumber to provide a single spectrum for a particular section. For the temperature and fluorescence data, the transects were divided into sections approximately 3 km in length, and a spline was used to create a series of 512 points with 5 m sample spacing. An FFT was calculated on each series. The series were averaged separately for the stratified and the well-mixed portions of the transects. Transect GB37 was entirely within the well-mixed region, so that it did not have a stratified portion. Generally 3–5 sections were averaged to determine each spectrum. Variance spectra also were computed for all of the acoustic data collected on transects at the WMS, DS, and FMS.

RESULTS

The sites chosen for this study were in two physically distinct hydrographic regions of Georges Bank, which provided strong contrast in the vertical stratification of the water column. On the southern flank of the Bank, temperatures ranged from 6.0–7.5°C at the surface to around 4°C at the bottom. The water column at this site remained stratified during the period of the cruise despite a storm midway through the cruise that caused the mixed layer to extend to deeper depths of 15–20 m. The density difference over the water column was always greater than 0.3 σ_t units. In contrast, at the well-mixed site, temperatures ranged between 6.1 and 6.4°C, but were nearly constant with depth on a given profile and had a top to bottom density difference of less than 0.05 σ_t units. Thus, these were ideal locations to compare estimates of the variability of the physical properties of the water column with the distribution of biological properties. This section will begin with a description of the time-series changes in physical properties at the mooring site that are directly relevant to the spatial and temporal patterns observed in the acoustic records from the stratified region. An analysis of the acoustical patterns from both the long and short transects will follow in which contrasts will be made between the patterns in the stratified and well-mixed areas. Finally, comparisons will be made among the acoustic data sets and the biovolume data and zooplankton counts from the MOCNESS tows taken while the acoustic records were being made.

Changes in stratification during the experimental period

The moored time-series of hourly averaged temperature, salinity, and water density data showed the development of thermal and density stratification over the upper 20 m of the water column during the first four days (Fig. 2). Surface temperatures warmed from ~6°C to >7.5°C. The wind speed, measured by R.V. *Albatross IV* and included in Fig. 2, was low during this period. On May 25, a wind event, with speeds up to 12.9 m s^{-1} (25 kts), mixed the upper 15–20 m of the water column and lowered the surface temperatures. This was followed by another period of low winds which lasted until the end of the cruise.

The high-pass filtered (periods <40 min) temperature records from the SeaCat and Tpod

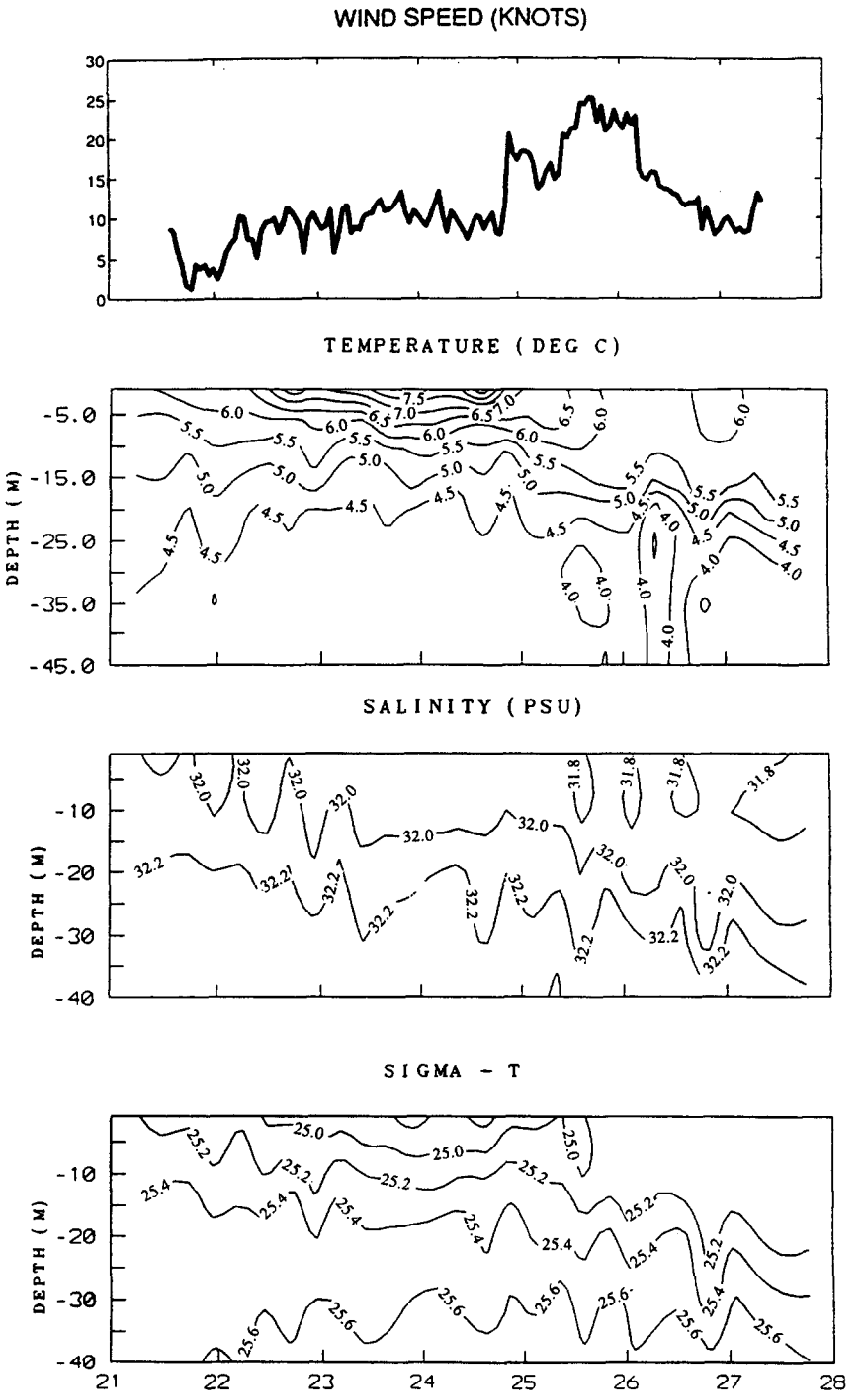

Fig. 2. Hourly average temperature, salinity, and σ_t time series from the mooring at the Fixed Mooring Site during the period 21–27 May 1992. Wind speed measured by *Albatross IV* is shown at the top.

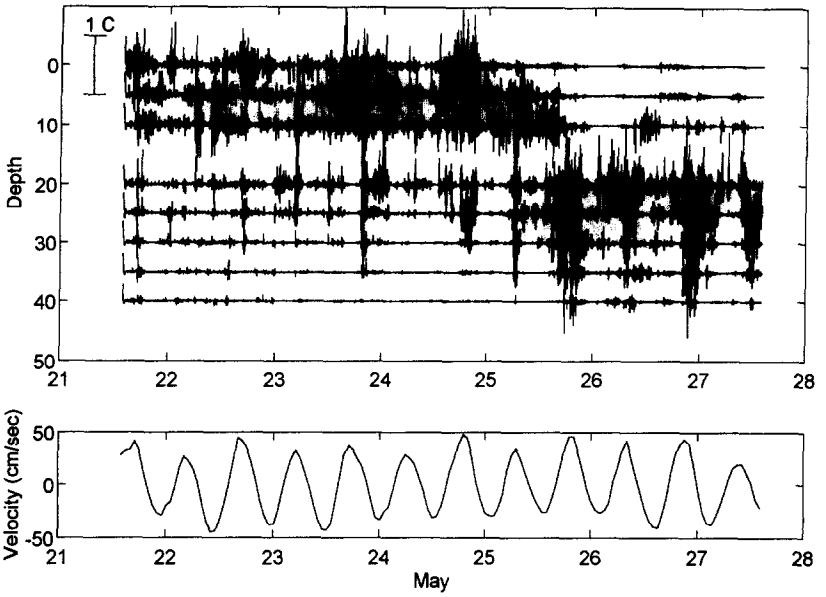

Fig. 3. High frequency temperature variability in the moored temperature records. The sampling interval is 2 min. The records are plotted at their location in the water column as indicated by the depth scale. The scale of temperature variability within each record is indicated by the vertical line in the upper left, which represents a range of 1°C. The cross-isobath current measured at the 15 m depth on the mooring is shown below the temperature records, with on-bank flow being positive.

instruments showed vertically coherent oscillations around the time of maximum on-bank tidal flow (Fig. 3). In the beginning of the record, this variability was evident in the upper 25 m; after the storm the variability was largest below 20 m depth. In both cases, the vertical temperature gradient was steepest in that portion of the water column. The variations represented internal waves with periods of about 15 min, as shown by an expanded plot of the variability on the afternoon of 26 May when the tide was flowing onto the Bank (Fig. 4a). The vertical amplitude of the oscillations was about 10–15 m.

The mooring data indicated that although some mixing occurred in the upper 10–15 m during the storm, the water column can be considered continuously stratified during the period that internal waves were observed. Given that the period of the observed oscillations was much shorter than the inertial period, the dispersion relation for internal waves [Munk, 1981, equation (9.4)]

$$\kappa^2 = \frac{-m_j^2\omega^2}{\omega^2 - N^2} \tag{2}$$

can be rewritten in terms of κ, the wavenumber of the waves: where $m_j = j\pi/H$ ($j = 1,2,3,...$), H is the water depth, ω is the frequency of the oscillations, and N is the Brunt–Väisala frequency. For the observed periods of about 15 min and the observed density structure, the wavelengths of the first mode ($j = 1$) internal waves would be on the order of 250–300 m. The existence of such waves was evident in a time-series acoustical record taken during a 3.5 h period on 26 May (year-day 147; Fig. 4b) and was also evident in the along-track acoustical data presented below.

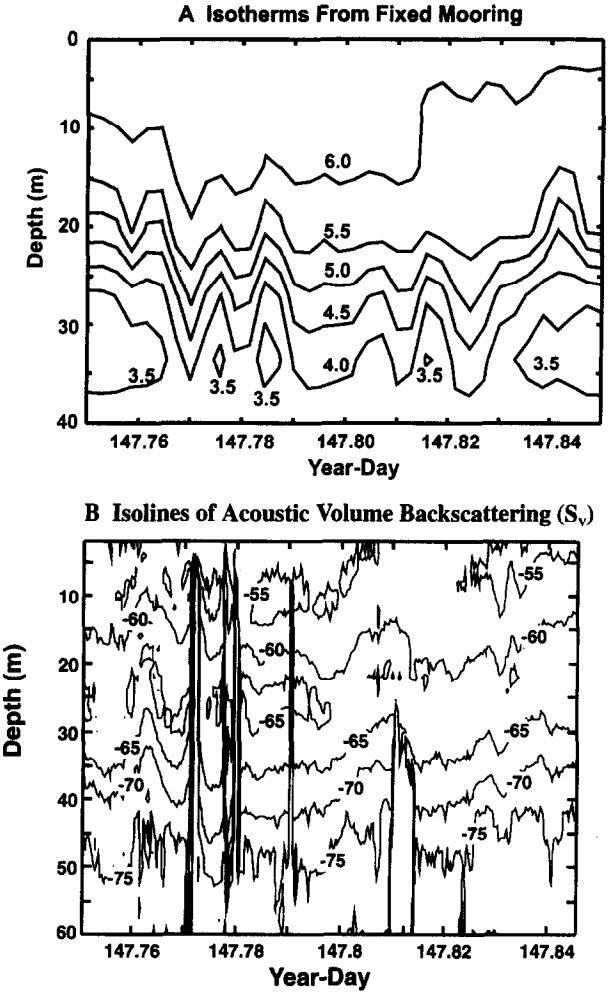

Fig. 4. (A) Moored temperature profile during on-bank current on 27 May; data averaged at 2 min intervals. (B) Towed body acoustical time-series record made during the on-bank current phase of the tide at the Fixed Mooring Site on 27 May while the ship maintained position near the mooring. The time base, year-day, is the sequential number of days (and fractions of a day, i.e. 0.01 year-day units corresponds to 14.4 min) in a year with day 1 equal to 1 January 1992.

Long acoustic transects across the hydrographic regimes

A striking feature of the acoustic transects across the Bank's hydrographic regimes (GB31 and GB36) was the substantially elevated level of volume backscattering at the FMS and DS (stratified region) relative to the WMS (approximately a factor of 5; Figs 5 and 6A,B). In addition, there were major differences in the vertical distribution of the scatterers in these two regions with pronounced stratification of the scatterers at mid-depths or the surface of the FMS and DS, and little or no stratification of the scatterers at the WMS. On both long transects, an abrupt transition (4–6 km) between the two regions was observed that marked the tidal mixing front. For the transect between the FMS and WMS (GB31), this

discontinuity occurred about midway along the track line at a depth of 60 m (Fig. 5). For the western transect (GB36), it occurred about two-thirds of the way along the track line in about the same depth of water (Fig. 6A). In the stratified region on GB31 (Fig. 5), three major acoustic patch structures were observed that had horizontal length scales of 500 m to 1500 m. On this transect, a large 4 km wide fluorescence peak, not associated with the acoustic backscattering field, occurred in the near-surface layer of the frontal region. Several large acoustic patches (length scales of 2000–5000 m) also were encountered on GB36 in the stratified area. Since both long transects cut across the isobaths and across the along-bank westward mean current flow, it is not known how extensive the acoustic patches were in a direction perpendicular to the transects. It is possible that they had an even larger horizontal extent parallel to the flow field.

The acoustic system was towed perpendicularly to the axis of the Great South Channel on a bright sunny day, when there was no wind, the sea was calm, and the sky was cloudless. The pattern of volume backscattering, which lacked vertical stratification, showed irregular, but consistent vertical striations of alternating high and low volume backscattering that went from the surface to near the bottom (water depth $\sim$70 m; Fig. 6B). This coherent pattern of fine-scale vertical lineations was observed along the entire transect. The horizontal spacing between the highs was about 50–100 m. At one point in the section, the concurrent towyoing with a CTD equipped with a fluorometer was adjusted to horizontal towing at 30 m in order to search for similar patterns. Temperature and salinity were isothermal ($\sim$6.5°C) and isohaline (32.30 psu), respectively, but fluorescence fluctuated markedly, showing regular spikes at intervals of 5–15 m. The short fluorescence record at 30 m depth in Great South Channel indicated that there was horizontal structure on scales smaller than can be resolved in the present acoustic data records. Analysis of acoustic records with shorter averaging times will be required in the future to determine if there is variability on similarly short scales in the acoustic backscattering fields.

Short transects within hydrographic regimes

During a 48-h period, acoustic transects were made at each of the three study sites at 6 h intervals to examine the extent to which patterns in volume backscattering could be replicated and were related to the physical structure of the water column. They also enabled examination of diel vertical migration behavior. Transects made in conjunction with CTD towyos were about 10 km long; those made with MOCNESS tows were of shorter distance (3–6 km; Figs 7–9).

The differences between the stratified and well-mixed areas observed on the long transects described above were replicated on the shorter ones. They provided clear evidence that physical forcing and biological responses to it were very different between the two areas.

At the stratified sites, there was pronounced vertical stratification and horizontal patchiness in the acoustic records. Average volume backscattering between the surface and 40 m was about 1.5 times higher at the DS than the FMS (Table 3). The standard deviation in the acoustical records was computed depth-bin-by-depth-bin to provide a vertical measure of variability, or row-by-row to provide a horizontal measure of variability. At both sites, the vertical variability was slightly smaller than the horizontal variability and coefficients of variation [$(s/\bar{x}) \times 100$—Sokal and Rohlf (1981)] ranged from 49% to 154%.

As on the long cross-shelf transects, intense subsurface acoustical patches were observed

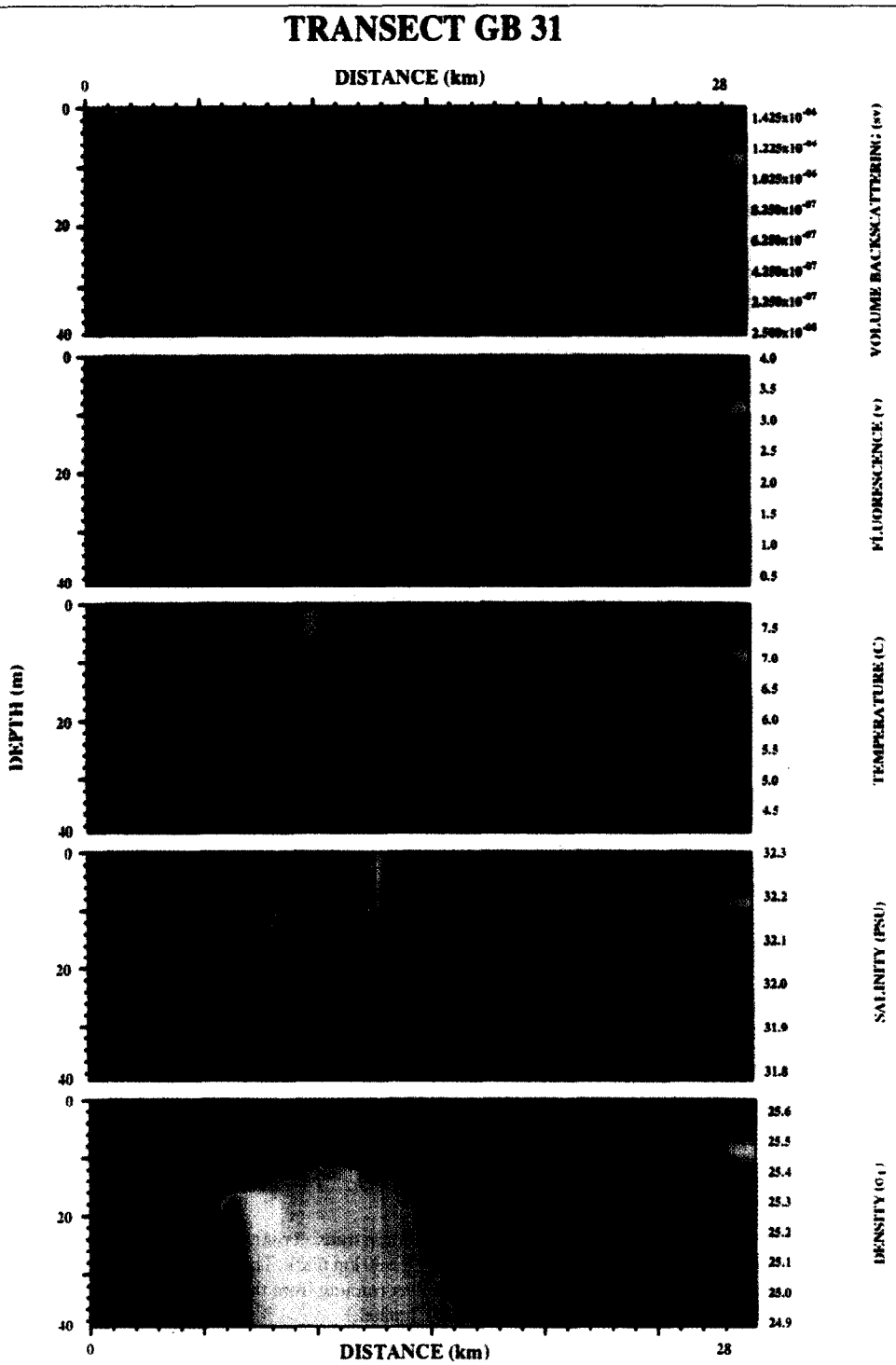

Fig. 5. Acoustical, biological, and physical structure along the transect between the Fixed Mooring Site (left side of panel) where the water was stratified and the Well-Mixed Site (right side of panel) where there was no stratification. Smoothed acoustic volume backscattering data (top panel) were collected from the 420 kHz acoustic system towed just below the surface. The fluorescence, temperature, salinity, and density data (panels 2–5) were collected by a CTD towyoed between the surface and the bottom while the ship steamed ahead at about 2.5 knots.

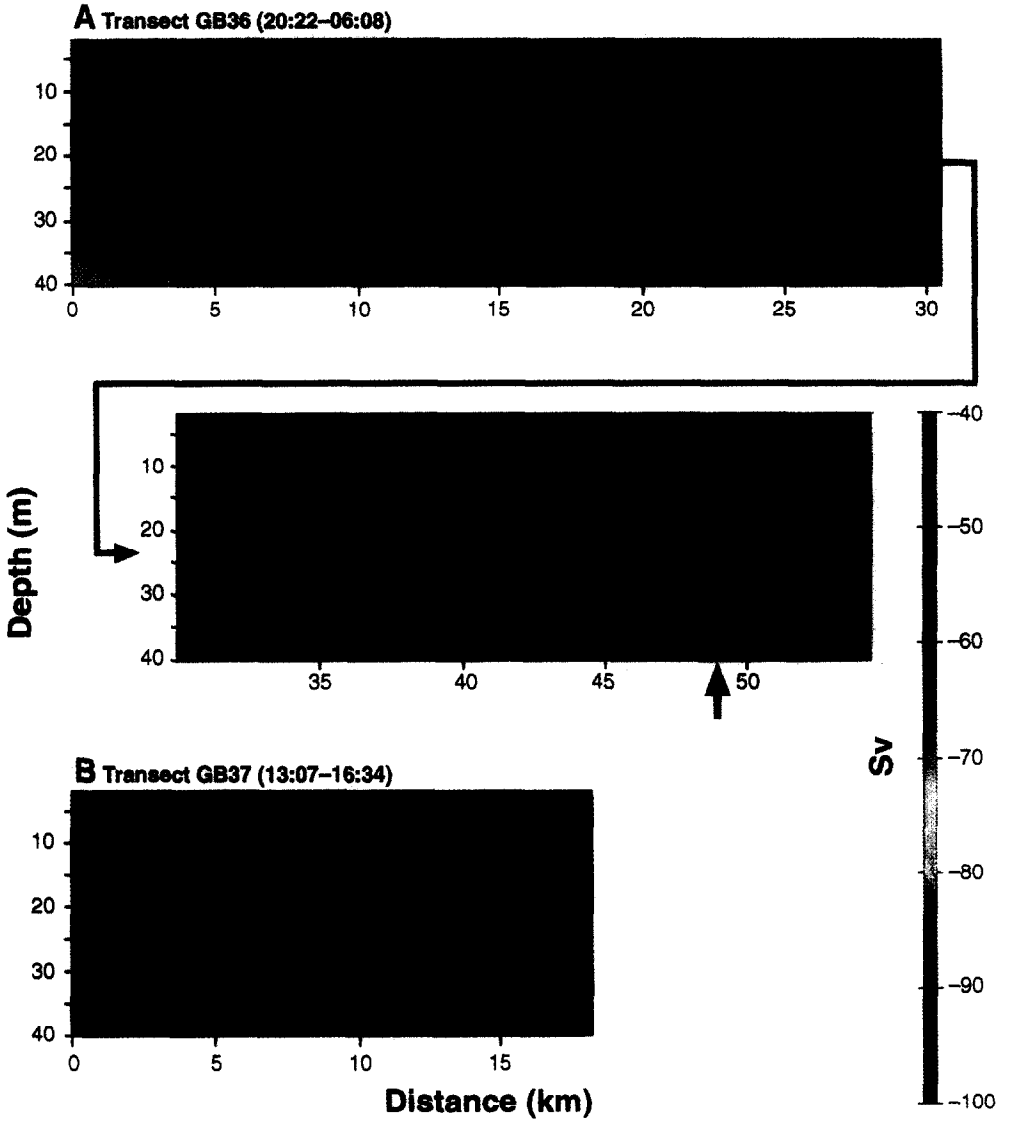

Fig. 6. (A) Acoustic records (upper 40 m) from the western transect running from the stratified area to the well-mixed area, which began at approximately the 30 km mark. The arrow marks sunrise. (B) Acoustic record (upper 40 m) from the acoustic transect running from the well-mixed area into the Great South Channel.

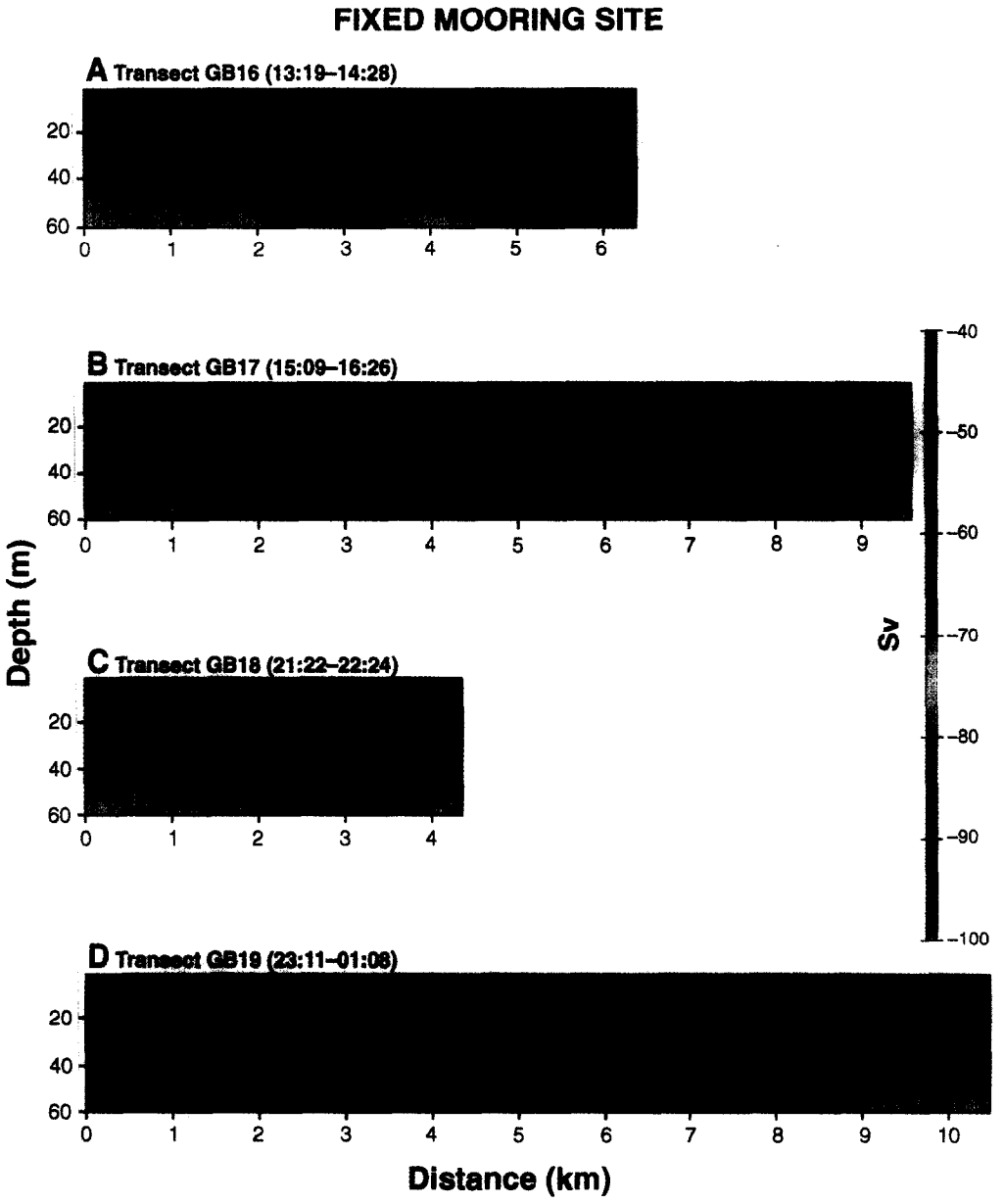

Fig. 7. Acoustic records from transects made at the Fixed Mooring Site. Local time of transect given next to transect number.

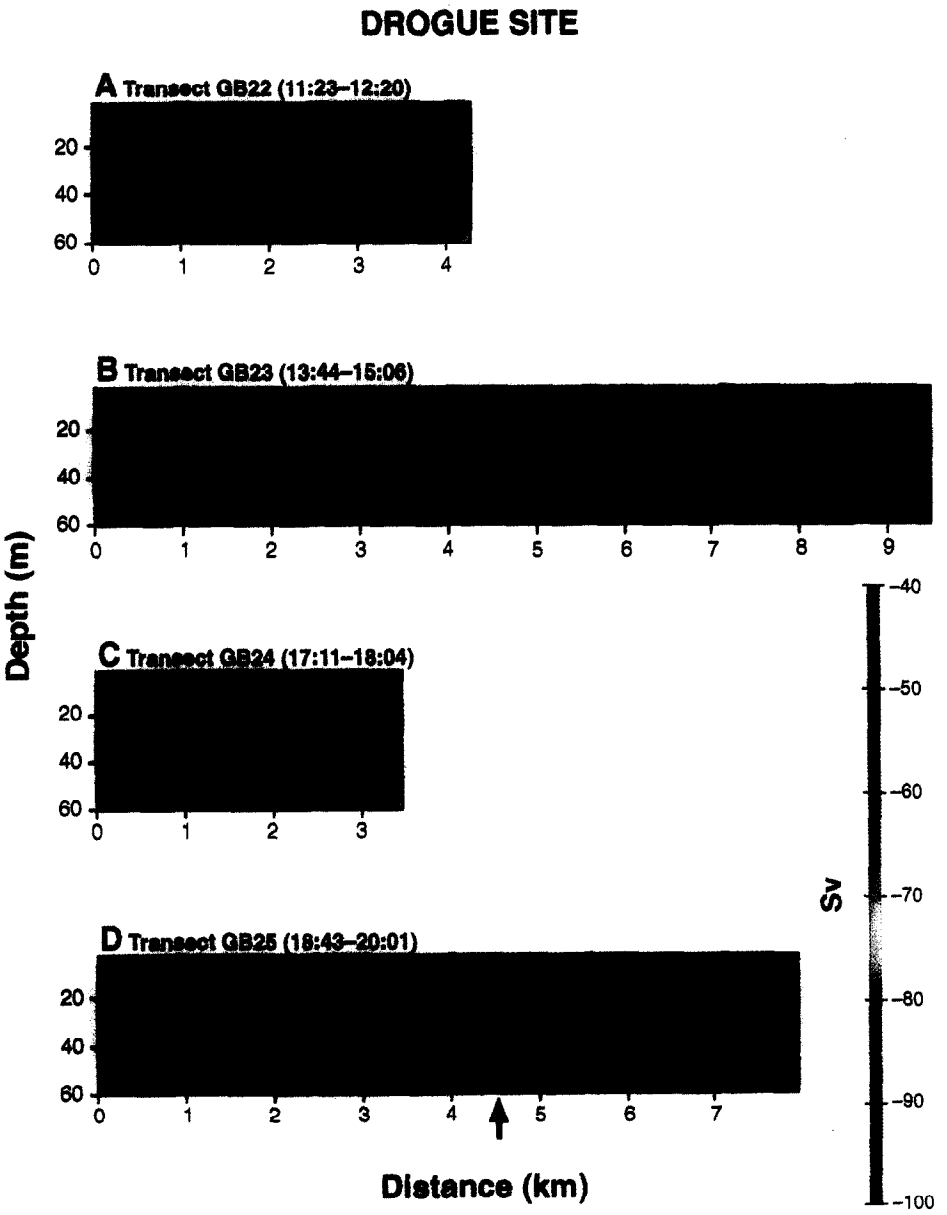

Fig. 8. Acoustic records from transects made at the Drogue Site. Local time of transect given next to transect number. The arrow marks sunset on transect GB25.

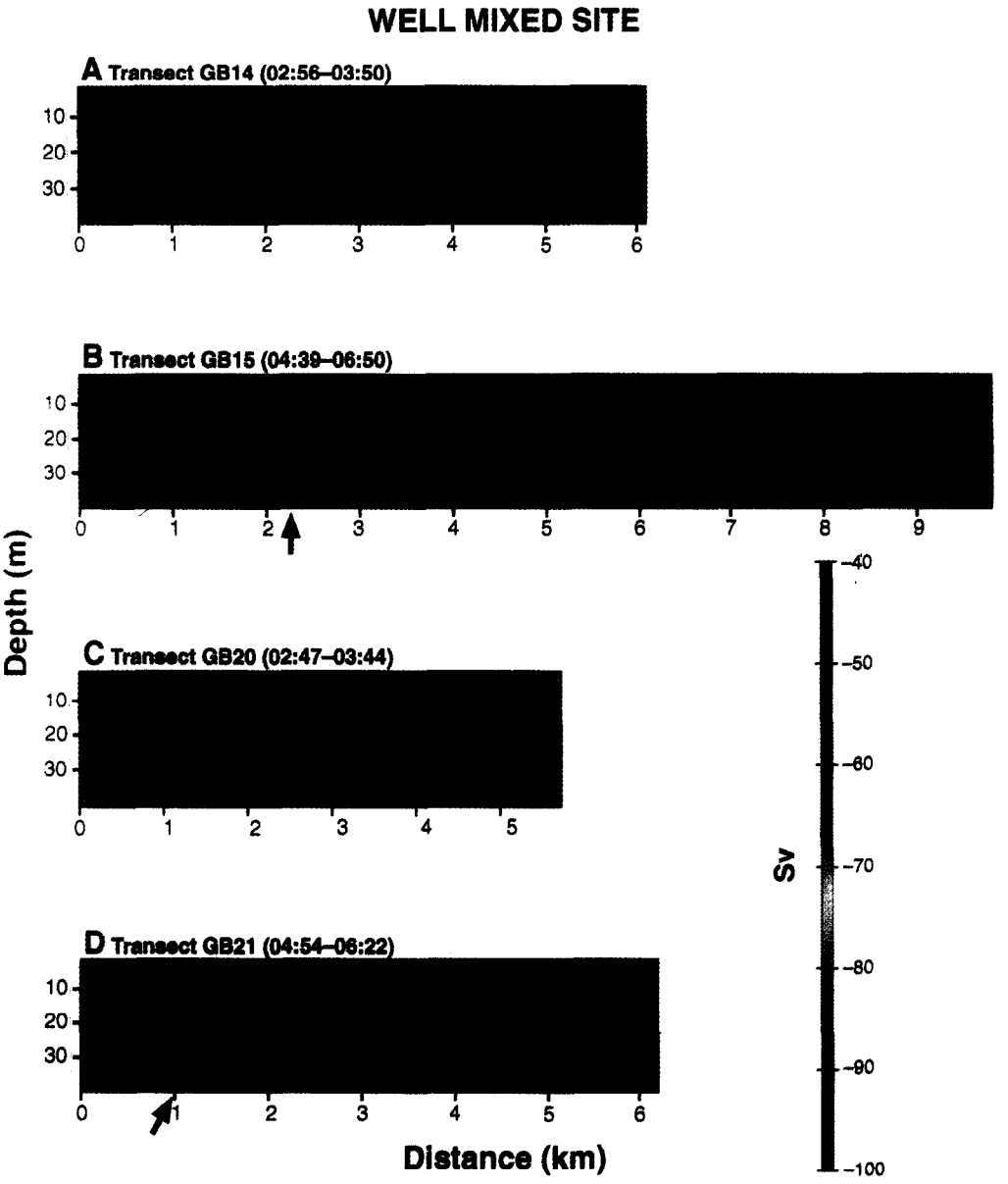

Fig. 9. Acoustic records from transects made at the Well-Mixed Site. Local time of transect given next to transect number. The arrows mark sunrise on transects GB15 and GB21.

Table 3. Summary of acoustic volume backscattering statistics for acoustic transects in the Fixed Mooring, Drogue, and Well-Mixed Sites, and MOCNESS biovolume data integrated for the 0–40 m water column

Tow number	Mean backscattering	Mean standard deviation*	Coefficient of variation $[(s/\bar{x}) \times 100]$*	MOCNESS tow no. biomass (mg/m^2)
Well-Mixed Site				
GB15	1.3e−7	4.7e−8v	35v	980 0.77
		2.5e−8h	17h	981 0.80
GB20	8.2e−8	6.0e−9v	7v	985 1.27
		4.9e−9h	6h	993 0.69
GB21	9.6e−8	1.7e−8v	17v	
		1.0e−8h	11h	
Fixed Mooring Site				
GB16	4.8e−7	2.7e−7v	76v	977 0.43
		3.5e−7h	74h	992 0.66
GB17	3.9e−7	3.0e−7v	73v	995 0.68
		4.0e−7h	99h	
GB18	4.0e−7	1.9e−7v	54v	
		3.4e−7h	90h	
GB19	5.0e−7	3.4e−7h	1.30v	
		4.5e−7h	91h	
Drogue Site				
GB22	7.6e−7	3.5e−7v	49v	982 1.01
		4.9e−7h	65h	984 0.84
GB23	6.4e−7	2.7e−7v	51v	987 0.56
		4.8e−7h	76h	990 0.94
GB24	7.3e−7	3.1e−7v	50v	
		5.1e−7h	78h	
GB25	7.4e−7	1.3e−6v	1.54v	
		5.4e−7h	63h	

*v indicates computation on vertical data; h indicates computation on horizontal data; s is the standard deviation; biomass units are wet weights.

on nearly all the transects made at the FMS and DS. They had horizontal lengths of 200–2000 m and vertical extents of 10–20 m. On several of these transects, very intense echoes were recorded (Fig. 8, GB24 and GB25). These acoustical structures were small (10s of meters) compared to the structures described above and were probably from fish schools, possibly herring.

Some of the horizontal variation of the acoustic backscatter at mid-depth appeared to be periodical, suggesting internal wave motion similar to that observed in the moored temperature records (Fig. 4A). For example, at mid-depths, the acoustic data from transect GB23, conducted during the on-bank tide the afternoon of 23 May showed vertical variations in horizontal s_v isolines of about 10 m, with length scales of 200–300 m (Fig. 8). There was no clear evidence of diel vertical migration behavior of the layers at the fixed mooring and drogue sites.

At the Well-Mixed Site, there was little horizontal layering and little in the way of coarse-scale horizontal structure, except at dawn (Fig. 9). However, the same fine-scale vertical

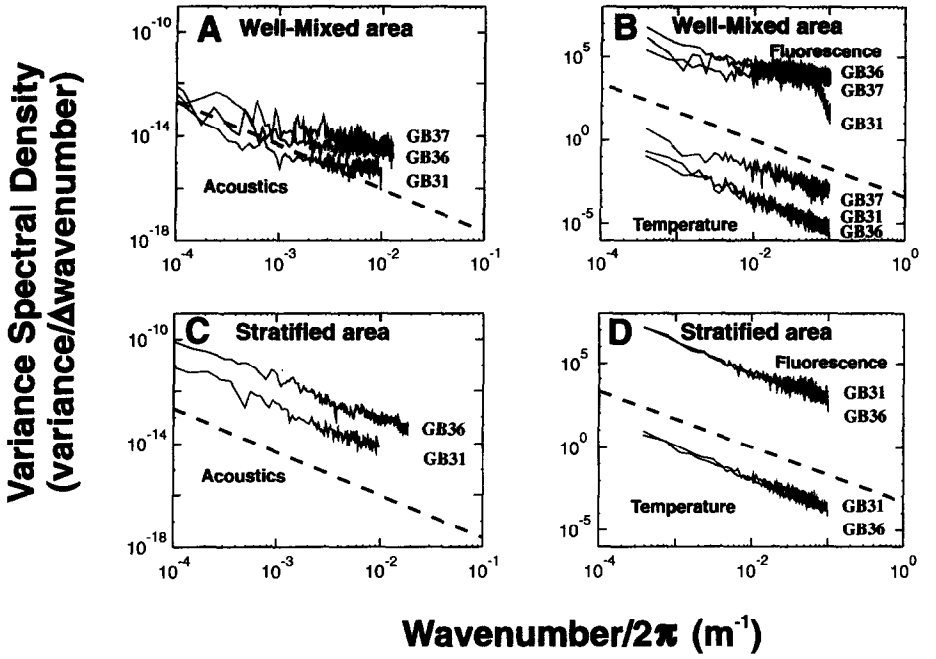

Fig. 10. (A) Variance spectra for acoustic space series from well-mixed portion of transects GB31 and GB36 and for transect GB37. (B) Variance spectra for temperature and fluorescence series from well-mixed portion of transects GB31 and GB36 and for transect GB37. (C) Variance spectra for acoustics series from stratified portions of transects GB31 and GB36. (D) Variance spectra for temperature and fluorescence series from stratified portions of transects GB31 and GB36. The dotted line has a $-5/3$ slope which is the expected slope of a spectrum in which turbulent mixing is a controlling force (see Discussion for additional detail). Wavenumber $= 2\pi/\lambda$, where λ is the spatial wavelength.

lineations observed on the portions of the long transects taken in the well-mixed region, were evident in all of the acoustical records collected on short transects at the Well-Mixed Site. The length-scale of this horizontal structure is on the order of the water column depth. Average volume backscattering between the surface and 40 m was between a factor of 4 and a factor of 7 lower than at the FMS and the DS (Table 3). The variability in the acoustical records from the WMS was lower by about an order of magnitude; the coefficients of variation ranged from 7% to 35%. At this site, the vertical variability was higher than the horizontal variability (Table 3).

On the two WMS transects that spanned dawn, there was a period of decreased volume backscattering shortly after the sun rose above the horizon (about 05:08 EDT; Fig. 9). The change was about a factor of two. On both occasions, the development of a "dawn hole" began at mid-depth and then extended towards the surface. It eventually encompassed most of the water column before volume backscattering values returned to the predawn levels. There was a subtle shift of the volume backscattering level, from being higher near the surface before dawn to higher near the bottom after dawn. We postulate that the "dawn hole" in backscattering may be due to a change in orientation of principal scatterers during a downward migration at dawn.

The variance spectra of the acoustical and non-acoustical along-track data collected by

the towed acoustic system provide another view of the horizontal structure in the stratified and well-mixed regions (Fig. 10A–D). Spectra were calculated for the stratified and well-mixed portions of transects GB31 and GB36, and for GB37, which was in the well-mixed region. All of the temperature spectra from the five sections (two in the stratified area and three in the well-mixed area Fig. 10 B,D) showed an approximate $-5/3$ slope. The spectra from the stratified portions of GB31 and GB36 (Fig. 10D) also showed the $-5/3$ slope. The fluorescence spectra from the well-mixed region (Fig. 10B) showed a decrease at the longer wavelengths of approximately $-5/3$. At higher wavenumbers, however, corresponding to wavelengths of less than about 250–300 m, the spectra broke from the $-5/3$ slope and had near-constant amplitude up to wavenumbers corresponding to wavelengths of less than 50 m. The acoustics data had a pattern similar to that of the fluorescence data. The acoustics variance spectra from the stratified portions of GB31 and GB36 (Fig. 10C) showed the $-5/3$ slope, but those from the well-mixed area deviated strongly from a $-5/3$ slope at wavelengths of less than 1000 m. At these shorter wavelengths, the spatial variability was essentially constant. Variance spectra computed for transects at the FMS, DS, and WMS showed the same pattern.

Although the fluorescence and acoustic variance spectra were both "white" in the well-mixed area, there was a difference in the changes in overall variance between the stratified and well-mixed areas. For the acoustical data, the variance at a given wavenumber was lower in the well-mixed area. However, the variance in the fluorescence data in the well-mixed area was equal to or substantially higher at the higher wavenumbers.

Biological interpretation of acoustic data

In spite of the fact that there was about a factor of 4–7 times difference between volume backscattering coefficient at the (stratified) Fixed Mooring and the Drogue Sites compared with the Well-Mixed Site, there was no significant difference in the net-collected zooplankton biovolumes between these two regions (Table 3). The low correlation between acoustic backscattering values and MOCNESS biovolumes was particularly evident when the volume backscattering associated with each net was compared to its biovolume using functional regression (Ricker, 1973; Fig. 11A). If the data are segregated by area (stratified versus well-mixed) and then analyzed, the functional regression relationship is improved, although the correlation for each comparison is still quite poor (Fig. 11B). At the Well-Mixed Site, a given level of MOCNESS biovolume corresponded to a lower level of volume backscattering than in the stratified areas regardless of biovolume level. As will be shown below, there were subtle changes in the composition of the plankton between the two regions which caused the differences in the acoustic levels.

The taxonomic composition of the 21 MOCNESS samples subjected to silhouette analysis showed that all of the areas sampled by the MOCNESS were dominated by copepods; they accounted for 75% to 95% of both the biomass and the numbers of individuals (Fig. 12A,B). In the stratified areas, the next most abundant taxon was the pteropod, *Limacina retroversa*. This species accounted for up to 25% of the biomass and numbers in the specific parts of the water column where it was most abundant (10–40 m). At the Well-Mixed Site, however, *L. retroversa* occurred in substantially lower numbers and biomass. Other taxonomic groups that contributed to most of the numbers and biovolume in the samples were chaetognaths, amphipods, euphausiid furcilia, and fish larvae (Fig. 12A,B). Chaetognaths contributed more to the biomass at the WMS; they were found in low

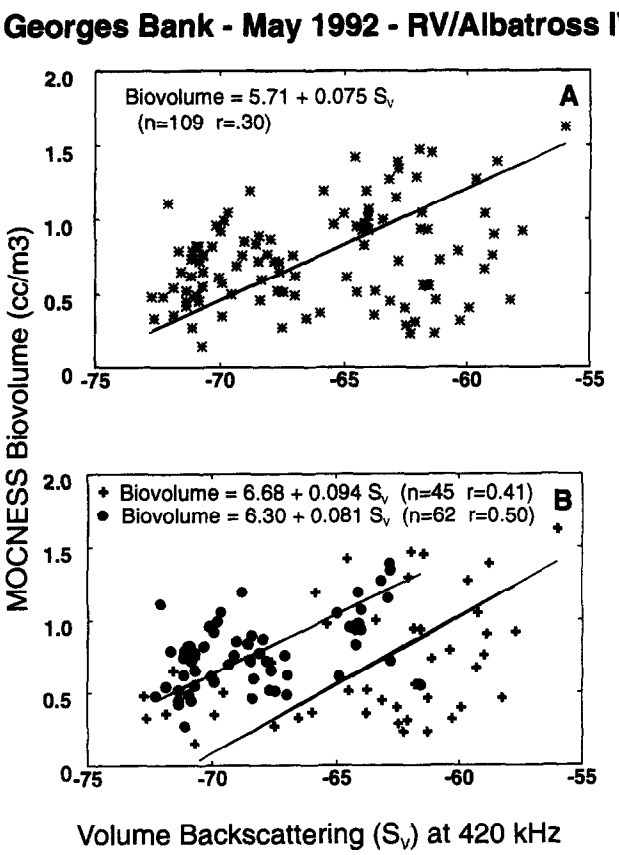

Fig. 11. The relationship between volume backscattering and MOCNESS biovolume: (A) all data combined; (B) data segregated by stratified and well-mixed regions of Georges Bank.

numbers in the stratified areas. The other taxa were present in both areas, but in general, their numbers and biomass were low.

The volume backscattering coefficient (s_v) is directly related to a combination of the numerical abundance of the sound scatterers present causing the reverberation and their individual scattering properties (Clay and Medwin, 1977). In this case, however, functional regression analysis revealed a significant relationship ($p<0.05$) between numbers of individuals and volume scattering only for pteropods and euphausiid larvae (Fig. 13). Copepods, chaetognaths, fish larvae, and amphipods were not significantly correlated with volume scattering. It is clear that numerical abundance of most taxa alone does not explain the observed volume backscattering levels.

ANALYSIS AND DISCUSSION

Physical structure and impact on biological records

One hypothesis to explain the vertical lineations in the well-mixed areas involves the development of secondary vertical circulation cells within the boundary layer associated

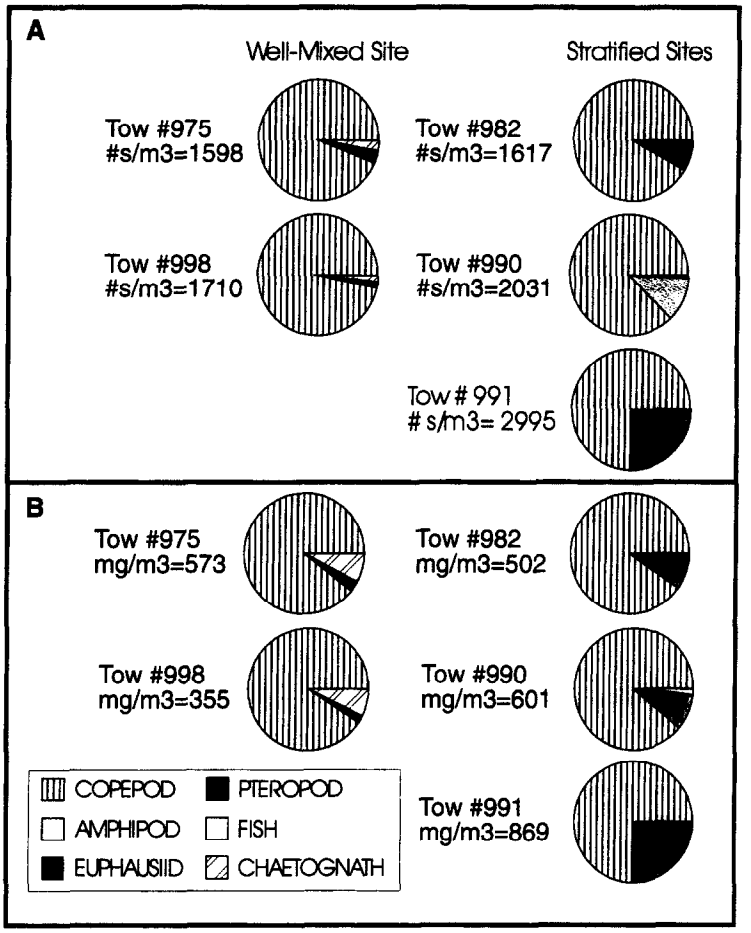

Fig. 12. Taxonomic composition of the plankton collected with a MOCNESS from the stratified and well-mixed areas of Georges Bank. Both numbers/m^3 and biomass (mg wet weight/m^3) are shown.

with the tidal flows over a rough bottom (Viekman *et al.*, 1989, 1992). These secondary flow cells, similar to Langmuir circulation cells set up by wind stress on the ocean surface, are organized, counter-rotating, helical vortices that give rise to convergences and divergences in a plane perpendicular to the direction of the predominant current. In the well-mixed area, the bottom boundary layer can reach to the surface, and it is conceivable that, in response to the continuous strong rotary tidal currents over dunes and ridges that are characteristic of much of the top of Georges Bank, secondary cells extend from the bottom to the surface most of the time. Such circulation cells by themselves, however, would not cause the variations in volume backscattering evident in our acoustical records. This hypothesis would require that the organisms have directed vertical motion. Passive movement with the secondary circulation cells would not produce the observed distributions (for Langmuir circulation, see Stavin, 1971; George and Edwards, 1973). Zooplankton scatterers attempting to maintain their position in the water column would be concentrated in the divergence portion of the cells by swimming downward and in the convergence portion of

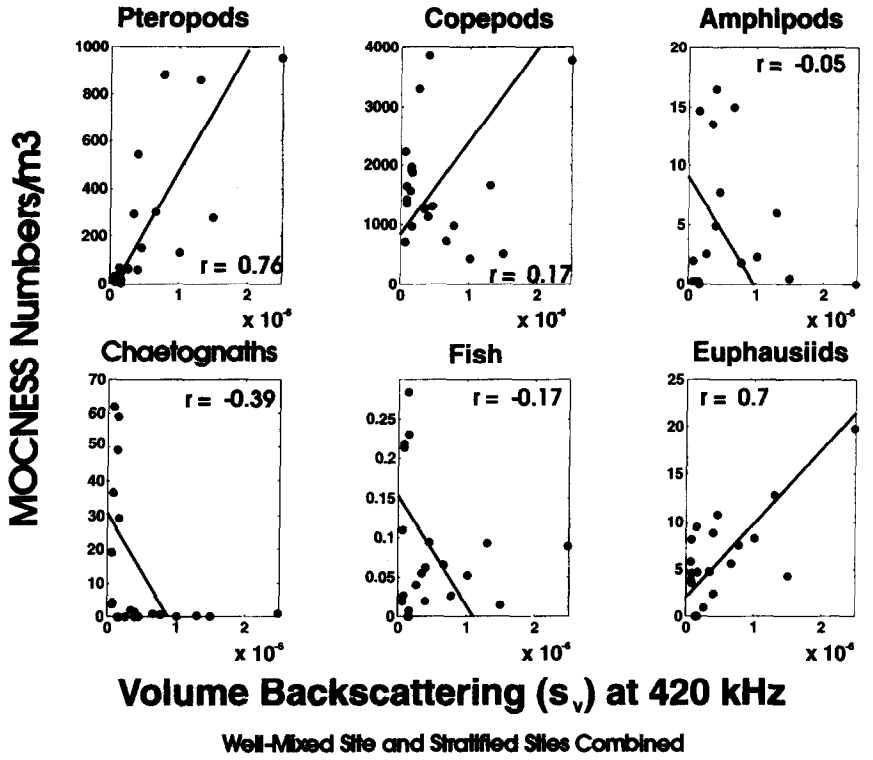

Fig. 13. The relationship between volume backscattering and abundance of taxonomic categories collected by 335 μm MOCNESS nets.

the cells by swimming upwards. In order for the fluorescence to show a patchiness pattern on these sampling scales, phytoplankton cells must also exhibit behavior that counters the direction of the physical forcing of the flow. We postulate that in the well-mixed region of the Bank, species that contribute significantly to the fluorescence signal are positively buoyant and tend to aggregate in convergence zones associated with downward-flowing portions of secondary circulation cells.

The $-5/3$ slope in the spectra of the along-track acoustic, temperature, and fluorescence data in the stratified area suggests that the spatial structure of the variability in these parameters was similar to that which would be caused by the strong turbulent mixing on the Bank. In a turbulent flow regime, the turbulent energy spectral density function characteristically is proportional to $\kappa^{-5/3}$ (where κ is the wavenumber) in a range of wavenumbers between the scales of turbulent generation and of dissipation. Plotted on a log–log axis, the spectrum in this range (often called the inertial sub-range) has a slope of $-5/3$ (Tennekes and Lumley, 1972). Other properties of the fluid (e.g. temperature or chlorophyll) often exhibit a slope of approximately $-5/3$ in their spectrum, suggesting that the distribution of their variance by length scale is controlled by the physical processes of turbulent mixing (e.g. Denman, 1976; Fasham and Pugh, 1976). While the processes controlling spectral shape generally are not that simple (e.g. see Platt, 1978), the $-5/3$ slope is a convenient reference by which to compare and differentiate spectra. The departure of the acoustic and fluorescence spectra in the well-mixed region from the $-5/3$ slope suggests that

other processes are occurring at the higher wavenumbers (shorter wavelengths), such as the secondary cell circulation. Townsend (1976) showed that for cell circulations associated with variations in surface (or bottom) roughness, there is a length scale above which the cells would not be self-sustaining. This upper limit on cell size is approximately four times the boundary layer thickness. Viekman *et al.* (1992) suggested from their observations a value of six times the layer thickness. In the well-mixed region of Georges Bank, the boundary layer is approximately the water depth, so the upper limit on cell size would be expected to be at about 250 m to 300 m. This is approximately the length scale at which the acoustic and fluorescence spectra in Fig. 10 break from the $-5/3$ slope. In the stratified region, the near surface layer would be isolated by the pycnocline from the bottom generated cell structure. There is some evidence in the acoustical records that under the pycnocline in the stratified region of the Bank, secondary circulation cells exist as well, but the deep acoustical records are not of sufficient quality to demonstrate this quantitatively.

Much larger "band like patterns" in satellite coastal zone color scanner (CZCS) images were observed by Yentsch *et al.* (1994) in the well-mixed region of Georges Bank, principally during the spring and summer months. These color bands, 5–10 km wide and 50–100 km long, appeared to be related to the bottom topography, as were ship measurements of sea surface temperature and chlorophyll. Because Yentsch *et al.*'s (1994) shipboard sampling interval (5 min and $\sim$1.4 km) was much larger than ours, the smaller-scale structures observed in our data sets could not be evident in their data. Nevertheless, they suggested that the same mechanism, namely secondary cell circulation caused by flow over a rough bottom, was the likely explanation for the existence of the larger structures.

The internal wave patterns evident in the moored current meter data from the stratified regions do not include the large, internal soliton-like features observed on the more energetic northern flank of the Bank (Brickman and Loder, 1993). The internal Froude number for the southern flank is about 0.8–1.0, much less than the value of three estimated by Loder *et al.* (1992) for the northern flank, and thus generation of soliton-like features would not be expected. The internal waves observed in the mooring records could represent an important process for enhancing cross-pycnocline mixing. More importantly, with 10–15 m amplitudes and periods of around 15 min, the existence of the waves needs to be considered when analyzing observations made during the peak of the on-bank tidal flow, particularly when comparing observations and samples from different instrument systems and collected at slightly different times. The acoustic records, however, occasionally show much larger, more energetic wave-like structures (Fig. 7, GB16).

Scattering model interpretation of acoustic records

Recent experimental laboratory work on the acoustic scattering properties of various zooplankton anatomical classes (Chu *et al.*, 1992; Stanton *et al.*, 1993; Stanton *et al.*, 1994) provides the foundation for this discussion about the low correlation between volume backscattering and MOCNESS biovolume data in the Georges Bank region. The pteropod contribution to the biovolume was moderate ($\sim$25%) in the stratified region and low ($\sim$5%) at the Well-Mixed Site, while the euphausiid furcilia contribution was small in both regions (Fig. 12). However, these two taxa were the only taxa out of a total of six that correlated with total s_v, indicating that pteropods and euphausiid furcilia may have contributed disproportionately to the volume backscattering. Our current understanding of the acoustical scattering properties of anatomical classes provides an explanation for this

phenomenon: the material properties of the animals varies substantially from class to class causing great changes in acoustic scattering levels, even for animals with the same biomass. For example, pteropods have hard shells and on a per-unit-biomass basis are orders of magnitude stronger acoustic scatterers (at 420 kHz) than other plankton types that have much softer bodies (See Table 1 in Stanton *et al.*, 1994). While few data for target strengths of live copepods have been published, their echo energy at 420 kHz is likely to be much lower than that of the pteropods; evidence is strong that their material properties are similar to that of the surrounding water (Greenlaw, 1977; Holliday *et al.*, 1989; Wiebe *et al.*, 1990). As will be shown below, despite a high correlation with the volume backscattering coefficient, the scattering predictions indicate that the euphausiids do not contribute strongly to the acoustic returns.

To approach the problem quantitatively, a set of equations was written to describe the partitioning of echo energies to each *j*th animal in each *i*th animal class, in the *k*th sample:

$$s_v^{(k)} = \frac{1}{V^{(k)}} \sum\sum < \sigma_{bs} >_{ij} \tag{3}$$

where $<\sigma_{bs}>$ is the "expected" backscattering cross section of an individual animal which is the backscattering cross section averaged over a number of pings during which time the animal is allowed to change shape (if appropriate) and orientation. $V^{(k)}$ is the volume of water sampled in the *k*th sample. In order for this equation using the expected cross-section to be valid, it must involve many pings over many animals, which was the case in this study.[1]

In order to estimate the relative contribution of the animals to the total acoustic energy, taxon-specific model equations given by Stanton *et al.* (1994) were used to estimate the size-specific acoustic backscattering cross-section of individuals at 420 kHz. Insertion of these estimated values (determined from silhouette analysis of net tow samples) for each individual animal in equation (3) produced predictions of $s_v^{(k)}$ that were compared with measurements of $s_v^{(k)}$. For this computation, the size frequency distribution in a cubic meter for each of the six taxonomic groups were determined from the silhouette analysis. These size data indicated that, except for the chaetognaths and fish, only minor changes in the sizes of the individual taxa occurred from region to region (Fig. 14). In terms of lengths, chaetognaths and fish larvae had the largest variation; copepods and pteropods were quite similar in size between the regions. Since few individuals were present that were gas-bearing (i.e. siphonophores), only two models were used. The dense fluid-sphere model was used for the pteropods, and the weakly scattering fluid-filled bent cylinder model was used for the other taxa (in the latter case, different sets of parameter values were applied depending upon taxa). The equations were taken directly from Stanton *et al.* (1994).

As evident in Fig. 15, the estimated pteropod contribution to the total volume

[1]In a first (unsuccessful) attempt to estimate the relative contribution of the animals to the total acoustic energy, the measured $s_v^{(k)}$ were entered into equation (3) leaving unknown the term $<\sigma_{bs}>_{ij}$. For 21 samples, this produced 21 equations with many more than 21 unknown values of $<\sigma_{bs}>_{ij}$. The equations were not solvable as they were under-determined. In order to proceed, the summation over *j* was replaced by a single value representing the sum over all animals in the *i*th taxon so that $<\sigma_{bs}>_{ij}$ was replaced by $<\sigma_{bs}>_i$, the backscattering cross-section averaged over size, shape (when appropriate), and orientation. Solution to this new set of equations via the non-negative least squares approach (Lawson and Hanson, 1974; σ_{bs} must remain non-negative) produced values for the mean cross-sections of the various animals. However, while the analysis revealed that pteropods accounted for most of the variance of s_v, it did not provide realistic estimates of backscattering cross-sections. It produced values of zero for the cross-sections of some of the taxa, a result which is not biologically plausible.

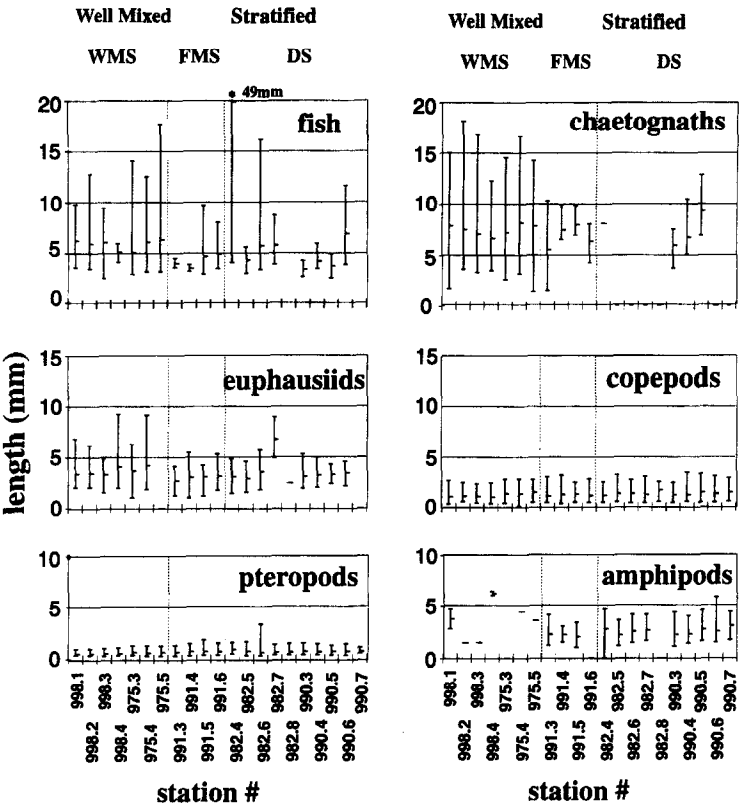

Fig. 14. Maximum, minimum, and mean size of individuals of the six major taxa contributing to the biomass of plankton in the MOCNESS samples collected in the stratified and well-mixed areas of Georges Bank.

backscattering is larger than that of any other taxon in many of the samples i.e. ≥ -60 dB. However, at lower s_v (≤ -60 dB), the other taxa, especially the copepods, appear to account for most of the volume backscattering. In a few samples, the model estimates indicate that chaetognaths can account for a substantial fraction of the backscattering. In contrast, in no samples do fish larvae, euphausiid larvae, or amphipods contribute in a major way to the estimated total backscattering. When the contributions of the other taxa are added to that of the pteropods, the relationship between the estimated total s_v and the measured s_v is significantly enhanced and very positively correlated ($r = 0.89$). The slope of the functional regression equation is nearly identical to the expected relationship (Fig. 15G).

While this result indicates that the backscattering models combined with field abundance estimates of the taxa can quantitatively predict trends in volume scattering, there are some important qualifications to be made. We have used the weakly scattering fluid-like model to characterize the individual volume backscattering of several taxa for which this model has not been experimentally demonstrated to be appropriate in laboratory studies (i.e. copepods, chaetognaths, and fish larvae). The weakly scattering fluid-like model appears reasonable, given what we now know about these species physical structure, but until laboratory experiments are conducted, this model's appropriateness will remain in question.

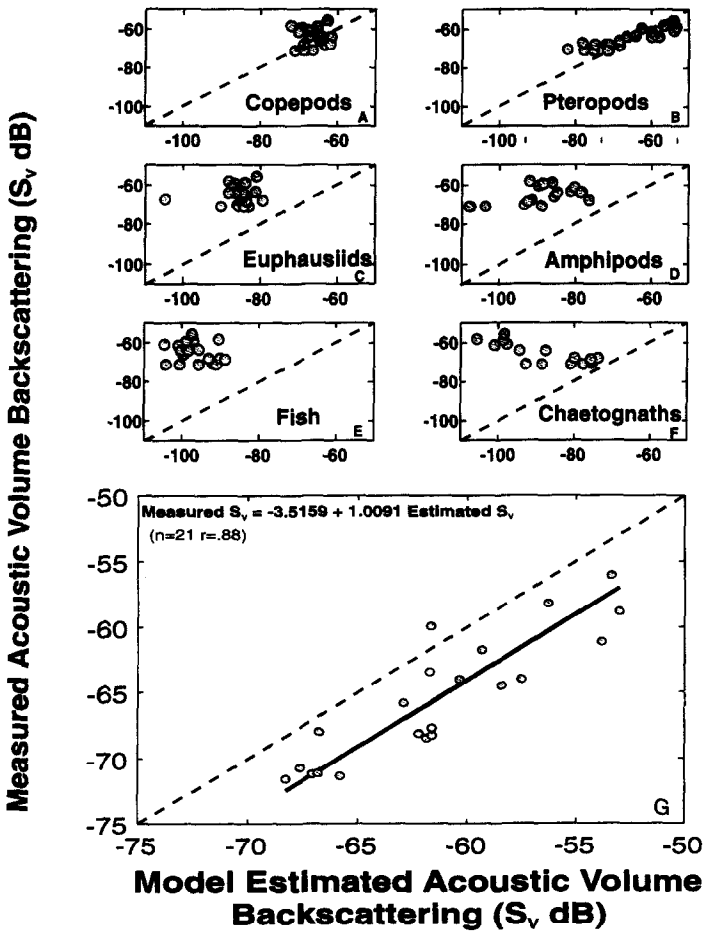

Fig. 15. (A)–(F) A comparison of estimated acoustic volume backscattering based on the mean size and abundance of the *individual* taxa in MOCNESS samples and the measured volume backscattering in the immediate vicinity of each net. Each plot represents the estimated contribution to the scattering by each group of animals compared with measurements of scattering by *all* animals types. (G) Total estimated acoustic volume backscattering based on the sum of the volume backscattering contributions estimated for each taxa in MOCNESS samples versus the measured volume backscattering for the net. The diagonal line is the expected line for an "ideal" comparison; the shorter line was determine with a functional regression (Ricker, 1973).

Furthermore, although the dense fluid sphere model used for the pteropods was based on laboratory data, the estimates should be considered as approximate. The Stanton *et al.* (1994) study reports significant variability (> 10 dB) in target strength levels between gastropods of similar size. A subsequent study (unpublished) where orientation was monitored suggests that at least some of this variability may be due to differences in orientation of the animals. If the animals in the ocean had a preferred orientation, the echo levels could easily differ by several decibels from a level averaged over all possible orientations. The remarkably good fit of the summed model estimates to the slope of the *in situ* measurements, however, demonstrates that a "first order" field test of these models

(collectively) is feasible and that the forward-modeling approach is a viable step in the quest to understand how to apply acoustics to study complex zooplankton assemblages in the field.

The patchiness structure revealed in this acoustical study is on smaller horizontal and vertical scales than that resolved by most conventional sampling gear and sampling schemes. In addition to being a very promising tool for studies of small-scale plankton patchiness, acoustical methods have unique properties for rapid broad-scale surveying. The high resolution necessary for patchiness studies is attained by ensonifying the water column several times per second. The broad-scale coverage necessary for survey work will result from being able to collect data at ship speeds of up to 8 kts. There is, however, the problem of interpreting the volume backscattering data in terms that are biologically meaningful. This study has shown that species composition can strongly influence the backscattering levels; thus a simple relationship between volume backscattering and plankton biovolume cannot be assumed. Knowledge of the acoustical scattering properties of the taxa making up the plankton will lead to new methods for gathering and interpreting volume backscattering data.

CONCLUSIONS

1. There are significant differences in overall levels of acoustic volume backscattering between the stratified and well-mixed regions of Georges Bank; on this occasion, the well-mixed regions had lower values.

2. The acoustic patchiness structure differed between regions: the stratified area had strong vertical gradients and intense horizontal structures; the well-mixed region had less intense, but persistent small-scale vertical lineations.

3. Variance spectra of the acoustical, temperature, and fluorescence data followed a $-5/3$ slope in the stratified region, but acoustical and fluorescence spectra deviated strongly from this slope in the well-mixed region of the Bank at wavelengths less than 1000 m. These "white" spectra indicated that factors other than turbulent energy dissipation were responsible for the fine-scale patchiness in well-mixed region.

4. Bank-wide, the correlation between volume backscattering and the biovolumes of plankton collected with a 1 m^2 MOCNESS was very low ($r = 0.3$), leaving most of the variability in the acoustical data unaccounted for.

5. Two taxon-specific models of acoustic backscattering cross-section were used with field-collected size and abundance data for zooplankton from net tows to predict volume backscattering data; these values were highly correlated with measured values. An important result was illustration of how the hard shelled gastropods that made up no more than 25% of the biovolume quite often dominated the acoustic echoes.

6. The fact that more than one set of model parameter values was needed to predict accurately volume backscattering indicates that more information about scattering properties of the animals are needed to transform measures of acoustical backscattering to meaningful biological variables. Knowledge of material properties is especially key in this analysis since the hard-shell gastropods were present in the aggregations of fluid-like animals.

Acknowledgements—We thank the officers and crew of the R.V. *Albatross IV* for skillful handling of the vessel and over-the-side equipment. We gratefully acknowledge that Arthur Allen of the U. S. Coast Guard (USCG) provided

the Loran C drifting buoy used in this study. We thank Jim Manning of the National Marine Fisheries Service (NMFS) who did the mooring data analysis and prepared Fig. 2. Linda Martin assisted with the acoustics data analysis, and Mark Benfield from the Louisiana State University and Ann Bucklin at the University of New Hampshire provided helpful comments. This work was supported by a National Oceanic and Atmospheric Administration (NOAA) grant NA16RC0515, Office of Naval Research grants NOOO14–89-J-1729, NOOO14–92-J-1527, and NOOO14–95-1–0287, National Science Foundation (NSF) grant OCE-801264 and the Woods Hole Oceanographic Institution. This is contribution number 8914 from the Woods Hole Oceanographic Institution and contribution number 57 of the U.S. GLOBEC program, funded by NSF and NOAA.

REFERENCES

Brickman D. and J. W. Loder (1993) Energetics of the internal tide on northern Georges Bank. *Journal of Physical Oceanography*, **23**, 409–424.

Chu D., T. K. Stanton and P. H. Wiebe (1992) Frequency dependence of sound backscattering from live individual zooplankton. *ICES Journal of Marine Science*, **49**, 97–106.

Clay C. S. and H. Medwin (1977) *Acoustical oceanography, principles and applications*. Wiley, NY.

Davis C. S. and P. H. Wiebe (1985) Macrozooplankton biomass in a warm-core Gulf Stream ring: Time series changes in size, structure, and taxonomic composition and vertical distribution. *Journal of Geophysical Research*, **90**, 8871–8884.

Denman K. L. (1976) Covariability of chlorophyll and temperature in the sea. *Deep-Sea Research*, **23**, 539–550.

Fasham M. J. and P. R. Pugh (1976) Observations on the horizontal coherence of chlorophyll *a* and temperature. *Journal Marine Research*, **34**, 593–601.

Flagg C. N. (1987) Hydrographic structure and variability, In: *Georges Bank*, R. H. Backus, editor, MIT Press, Cambridge, MA, pp. 108–124.

Garrett C. J. R., J. R. Keely and D. A. Greenberg (1978) Tidal mixing versus thermal stratification in the Bay of Fundy and Gulf of Maine. *Atmosphere–Ocean*, **16**, 403–423.

George D. G. and R. W. Edwards (1973) *Daphnia* distribution within Langmuir circulations. *Limnology and Oceanography*, **18**, 798–800.

Greenlaw C. F. (1977) Backscattering spectra of preserved zooplankton. *Journal of the Acoustical Society of America*, **62**, 44–52.

Holliday D. V., R. E. Pieper and G. S. Kleppel (1989) Determination of zooplankton size and distribution with multi-frequency acoustic technology. *Journal du Conseil Permanent International pour l'Exploration de la Mer*, **41**, 226–238.

Lawson C. L. and R. J. Hanson, (1974) *Solving least squares problems*. Prentice-Hall, Chapter 23.

Loder J. W., D. Brickman and E. P. W. Horne (1992) Detailed structure of currents and hydrography on the northern side of Georges Bank. *Journal of Geophysical Research*, **97**, 14,331–14,351.

Lough R. G. and D. C. Potter (1993) Vertical distribution patterns and diel migrations of larval and juvenile haddock, *Melanogrammus aeglefinus* and Atlantic cod *Gadus morhua*. *Fishery Bulletin*, **91**, 281–303.

Munk W. (1981) Internal waves and small-scale processes. In: *Evolution of physical oceanography*, B. A. Warren and C. Wunsch, editors, MIT Press, Cambridge, MA.

Parks T. W. and C. S. Burrus (1987) *Digital filter design*. John Wiley, Chichester, U.K.

Platt T. (1978) Spectral analysis of phytoplankton. In: *Spatial pattern in plankton communities*, J. H. Steele, editor, New York, pp. 73–84.

Ricker W. E. (1973) Linear regressions in fishery research. *Journal Fisheries Research Board of Canada*, **30**, 409–484.

Sokal R. R. and F. J. Rohlf (1981) *Biometry. The principals and practice of statistics in biological research*, W. H. Freeman and Co., New York, 859 pp.

Stanton T. K., D. Chu, P. H. Wiebe and C. S. Clay (1993) Average echoes from randomly-oriented random-length finite cylinders: zooplankton models. *Journal of the Acoustical Society of America*, **94**, 3463–3472.

Stanton T. K., P. H. Wiebe, D. Chu, M. Benfield, L. Scanlon, L. Martin and R. L. Eastwood (1994) On acoustic estimates of zooplankton biomass. *ICES Journal of Marine Science*, **51**, 505–512.

Stavin R. H. (1971) The horizontal–vertical distribution hypothesis: Langmuir circulations and *Daphnia* distributions. *Limnology and Oceanography*, **16**, 453–466.

Tennekes H. and J. L. Lumley (1972) *A first course in turbulence*. MIT Press, Cambridge, MA, 300 pp.

Townsend A. A. (1976) *The structure of turbulent shear flow*, Cambridge University Press, Cambridge, MA.

Viekman B. E., M. Wimbush and J. C. Van Leer (1989) Secondary circulations in the bottom boundary layer over sedimentary furrows. *Journal of Geophysical Research*, **94C7**, 9721–9730.

Viekman B. E., R. D. Flood, M. Wimbush, M. Faghri, Y. Asako and J. C. Van Leer (1992) Sedimentary furrows and organized flow structure: A study in Lake Superior. *Limnology and Oceanography*, **37**, 797–812.

Wiebe P. H. (1988) Functional regression equations for zooplankton displacement volume, wet weight, dry weight, and carbon: A correction. *Fishery Bulletin*, **86**, 833–835.

Wiebe P. H. and C. H. Greene (1994) The use of high frequency acoustics in the study of zooplankton spatial and temporal patterns. *Proceedings of the NIPR Symposium on Polar Biology*, **7**, 133–157.

Wiebe P. H., S. H. Boyd and J. Cox (1975) Relationships between zooplankton displacement volume, wet weight, dry weight, and carbon. *Fishery Bulletin*, **73**, 777–786.

Wiebe P. H., A. W. Morton, A. M. Bradley, R. H. Backus, J. E. Craddock, T. J. Cowles, V. A. Barber and G. R. Flierl (1985) New developments in the MOCNESS, an apparatus for sampling zooplankton and micronekton. *Marine Biology*, **87**, 313–323.

Wiebe P. H., C. H. Greene, T. Stanton and J. Burczynski (1990) Sound scattering by live zooplankton and micronekton: empirical studies with a dual-beam acoustical system. *Journal of the Acoustical Society of America*, **88**, 2346–2360.

Yentsch C. S., D. A. Phinney and J. W. Campbell (1994) Color banding on Georges Bank as viewed by coastal zone color scanner. *Journal of Geophysical Research*, **99C4**, 7401–7410.